Journal of Sound and Vibration (2001) **245**(1), 29–44
doi:10.1006/jsvi.2000.3544, available online at http://www.idealibrary.com on IDEAL®

FLOW-INDUCED VIBRATIONS OF SHEAR-DEFORMABLE LAMINATED PLATES EXPOSED TO AN OSCILLATING FLOW

L. Zhang, H.-S. Shen and J. Yang

School of Civil Engineering and Mechanics, Shanghai Jiao Tong University, Shanghai 200030, *People's Republic of China. E-mail: hsshen@mail.sjtu.edu.cn*

(*Received* 2 *June* 2000, *and in final form* 6 *November* 2000)

Using Reddy's higher order shear deformation plate theory, the flow-induced vibrations of simply supported shear-deformable laminated plates exposed to an oscillating flow are studied. The plate is assumed to be placed normal to the flow. The fluid–structure interaction is based on Morison's model, which leads to a non-linear motion equation. The state variable approach is used in conjunction with the Spline collocation method to determine the dynamic response of the plate. Numerical illustrations concern the dynamic response of antisymmetric angle-ply and symmetric cross-ply laminated plates under oscillating flow. The roles played by plate aspect ratio, total number of plies, fiber orientation, as well as transverse shear deformation are studied. In all cases, non-linear effects lead to rather complex vibrations and to essentially chaotic motion.

1. INTRODUCTION

Vibration of plate structures induced by oscillating flow occurs widely in practical engineering, for example, vibration of offshore platform structures induced by ocean waves. Flow over bluff bodies causes the development of separating flow and the vortex shedding behind the plate may be observed. The vortex patterns are somewhat different from the ordinary Kármán vortex street observed behind a symmetric bluff body in a uniform flow. Some numerical and experimental studies [1–5] on the prediction of fluid forces acting on and flow patterns behind inclined and normal plates in oscillating flow have already been reported. The laminated plate may vibrate in the transverse direction under the in-line fluid force, on placing the plate normal to the oscillating flow.

In spite of the practical importance of the problem, there is a need to have a better understanding of composite shear-deformable laminated plates exposed to an oscillating flow.

Many free vibration studies for composite laminated plates are available in the literature, see, e.g., references [6–16]. Numerous studies involving the application of the shear deformation plate theory to transient dynamic response of composite laminated plates can be found in references [17–20]. However, there is no literature dealing with the dynamic response of shear-deformable laminated plates exposed to an oscillating flow. This is the problem studied in the present paper for the case when all four edges of the plate are assumed to be simply supported with no in-plane displacement.

In the present study, the formulations are based on Reddy's higher order shear deformation plate theory [21]. The plate is assumed to be placed normal to the flow. The

0022-460X/01/310029 + 16 $35.00/0

fluid–structure interaction is based on Morison's model [22], which leads to a non-linear motion equation. The state variable approach (SVA) [18, 19] is used in conjunction with the Spline collocation method to determine the dynamic response of the plate. Numerical illustrations concern the dynamic responses of antisymmetric angle-ply and symmetric cross-ply laminated plates exposed to an oscillating flow.

2. EQUATIONS OF MOTION

Consider a rectangular plate of length a, width b and thickness h, which consists of N plies. The plate is subjected to a transverse distributed load, q, caused by oscillating flow. As usual, the co-ordinate system has its origin at the corner of the plate. Let u, v, w be the displacements parallel to the right-hand set of axes (x, y, z), where x is longitudinal and z is perpendicular to the plate. ψ_x and ψ_y are the rotations of transverse normals about the y- and x-axis, respectively, at the mid-plane. Let $F(x, y)$ be the stress function for the stress resultants, and denote differentiation by a comma, so that $N_x = F_{,yy}$, $N_y = F_{,xx}$ and $N_{xy} = -F_{,xy}$.

Attention is confined to the following two cases: (1) antisymmetric angle-ply laminated plates; and (2) symmetric cross-ply laminated plates, from which solutions for isotropic and orthotropic plates follow as a limiting case.

The deduction of the governing equations associated with Reddy's higher order shear deformation plate theory (HSDPT) follows the same pattern in the case of its static counterpart [23, 24], so that the motion equations of shear-deformable laminated plates can be written as

$$L_{11}(w) - L_{12}(\psi_x) - L_{13}(\psi_y) + L_{14}(F) = q - I_{11}\ddot{w} + I_{12}\left(\frac{\partial^2 \ddot{w}}{\partial x^2} + \frac{\partial^2 \ddot{w}}{\partial y^2}\right) + I_{13}\left(\frac{\partial \ddot{\psi}_x}{\partial x} + \frac{\partial \ddot{\psi}_y}{\partial y}\right), \tag{1}$$

$$L_{21}(w) + L_{22}(\psi_x) - L_{23}(\psi_y) + L_{24}(F) = I_{21}\frac{\partial \ddot{w}}{\partial x} + I_{22}\ddot{\psi}_x, \tag{2}$$

$$L_{31}(w) - L_{32}(\psi_x) + L_{33}(\psi_y) + L_{34}(F) = I_{31}\frac{\partial \ddot{w}}{\partial y} + I_{32}\ddot{\psi}_y, \tag{3}$$

$$L_{41}(F) + L_{42}(\psi_x) + L_{43}(\psi_y) - L_{44}(w) = 0 \tag{4}$$

in which a superposed dot indicates differentiation with respect to time, and operators $L_{ij}()$ and I_{ij} are defined in Appendix A.

All four edges are assumed to be simply supported, the boundary conditions are

$x = 0, a$:

$$u = w = \psi_y = 0, \qquad F_{,xy} = M_x = P_x = 0. \tag{5a}$$

$y = 0, b$:

$$v = w = \psi_x = 0, \qquad F_{,xy} = M_y = P_y = 0, \tag{5b}$$

where M_x and M_y are the bending moments, and P_x and P_y are the higher order moments respectively.

It is assumed that the plate is placed normal to the oscillating flow and the velocity of the fluid is parallel to the z direction.

As it has been shown by Morison [22], the in-line fluid force on the plate may be divided into two parts, one is drag force caused by unsteady velocity and the other is intertia force caused by acceleration or deceleration of the fluid. The fluid force per unit area is now defined by

$$q = q_I + q_D = \rho_0 \frac{A}{b} \ddot{U}(t) + c_I \rho_0 \frac{A}{b} (\ddot{U}(t) - \ddot{w}) + \frac{1}{2} c_D \rho_0 |\bar{\dot{U}} + \dot{U}(t) - \dot{w}| (\bar{\dot{U}} + \dot{U}(t) - \dot{w}), \tag{6}$$

where ρ_0 is the density of fluid, c_I the coefficient of added mass, c_D the drag coefficient, $\dot{U}(t)$ the fluid velocity as a function of time, $\bar{\dot{U}}$ the mean fluid velocity, and A the circular area whose diameter equals the width of the plate.

For the oscillating flow with zero mean, i.e. $\bar{\dot{U}} = 0$, equation (6) becomes

$$q = c_m \rho_0 \frac{A}{b} \ddot{U}(t) - c_I \rho_0 \frac{A}{b} \ddot{w} + \frac{1}{2} c_D \rho_0 |\dot{U}(t) - \dot{w}| (\dot{U}(t) - \dot{w}) \tag{7}$$

in which c_m is the inertia coefficient and $c_m = 1 + c_I$.

Substituting equation (7) into equation (1) yields

$$\begin{aligned} L_{11}(w) - L_{12}(\psi_x) - L_{13}(\psi_y) + L_{14}(F) = {} & c_m \rho_0 \frac{A}{b} \ddot{U}(t) - c_I \rho_0 \frac{A}{b} \ddot{w} \\ & + \frac{1}{2} c_D \rho_0 |\dot{U}(t) - \dot{w}| (\dot{U}(t) - \dot{w}) - I_{11} \ddot{w} \\ & + I_{12} \left(\frac{\partial^2 \ddot{w}}{\partial x^2} + \frac{\partial^2 \ddot{w}}{\partial y^2} \right) + I_{13} \left(\frac{\partial \ddot{\psi}_x}{\partial x} + \frac{\partial \ddot{\psi}_y}{\partial y} \right). \end{aligned} \tag{8}$$

It is noted that, if c_D is non-zero valued, equation (8) is a non-linear motion equation.

3. SOLUTIONS PROCEDURE

The dynamic response of a simply supported shear-deformable laminated plate under oscillating flow is now determined by using an analytical–numerical procedure. Firstly, the state variable approach (SVA) is used to solve equations (8), (2), (3) and (4), and we assume that

$$w(x, y, t) = \sum_{m,n=1}^{\infty} W_{mn}(t) \sin \alpha x \sin \beta y, \tag{9a}$$

$$\psi_x(x, y, t) = \sum_{m,n=1}^{\infty} X_{mn}(t) \cos \alpha x \sin \beta y, \tag{9b}$$

$$\psi_y(x, y, t) = \sum_{m,n=1}^{\infty} Y_{mn}(t) \sin \alpha x \cos \beta y, \tag{9c}$$

where $W_{mn}(t)$, $X_{mn}(t)$ and $Y_{mn}(t)$ are unknown functions.

Substituting equation (9) into equation (4), the solution of stress function satisfying the boundary conditions of equation (5) can be obtained as

$$F = \sum_{m,n=1}^{\infty} [g_1 W_{mn}(t) + g_2 X_{mn}(t) + g_3 Y_{mn}(t)] \cos \alpha x \cos \beta y, \tag{10}$$

where g_1, g_2 and g_3 are coefficients defined in Appendix B.

Substituting equations (9) and (10) into equation (8) yields

$$[K_{11} W_{mn}(t) + K_{12} X_{mn}(t) + K_{13} Y_{mn}(t)] \sin \alpha x \sin \beta y =$$

$$c_m \rho_0 \frac{A}{b} \ddot{U} - [M_{11} \ddot{W}_{mn}(t) + M_{12} \ddot{X}_{mn}(t) + M_{13} \ddot{Y}_{mn}(t)] \sin \alpha x \sin \beta y$$

$$+ \frac{1}{2} c_D \rho_0 |\dot{U} - \dot{W}_{mn}(t) \sin \alpha x \sin \beta y| (\dot{U} - \dot{W}_{mn}(t) \sin \alpha x \sin \beta y). \tag{11}$$

Making use of Galerkin's orthogonality condition, we have

$$M_{11} \ddot{W}_{mn}(t) + M_{12} \ddot{X}_{mn}(t) + M_{13} \ddot{Y}_{mn}(t) + f_1(t) W_{mn}(t) + a_1 \dot{W}_{mn}^2(t)$$

$$+ K_{11} W_{mn}(t) + K_{12} X_{mn}(t) + K_{13} Y_{mn}(t) = f_2(t) + f_3(t), \tag{12a}$$

where $f_1(t), f_2(t), f_3(t)$ and a_1 are defined in Appendix C. Note that now equation (12a) is a non-linear equation.

Similarly, from equations (2) and (3), we have

$$M_{21} \ddot{W}_{mn}(t) + M_{22} \ddot{X}_{mn}(t) + K_{21} W_{mn}(t) + K_{22} X_{mn}(t) + K_{23} Y_{mn}(t) = 0, \tag{12b}$$

$$M_{31} \ddot{W}_{mn}(t) + M_{33} \ddot{Y}_{mn}(t) + K_{31} W_{mn}(t) + K_{32} X_{mn}(t) + K_{33} Y_{mn}(t) = 0. \tag{12c}$$

The $[M_{ij}]$, $[K_{ij}]$ given in equation (12) are also defined in Appendix C.

Next, equation (12) can be solved by an increment method and can be written as

$$\bar{\mathbf{M}}(t) \Delta \ddot{\mathbf{Z}}_{mn} + \bar{\mathbf{C}}(t) \Delta \dot{\mathbf{Z}}_{mn} + \bar{\mathbf{K}}(t) \Delta \mathbf{Z}_{mn} = \Delta \mathbf{P}(t) \tag{13}$$

where $\mathbf{Z}_{mn} = \{W_{mn}, X_{mn}, Y_{mn}\}^{\mathrm{T}}$ is the displacement vector. $\bar{\mathbf{M}}(t)$, $\bar{\mathbf{K}}(t)$ and $\bar{\mathbf{C}}(t)$ are mass, stiffness and damping matrices, respectively, $\Delta \mathbf{P}(t)$ is the load increment vector, and the details can be found in Appendix D. Let the time increment be very small; then in each time increase step $\bar{\mathbf{M}}(t)$, $\bar{\mathbf{K}}(t)$ and $\bar{\mathbf{C}}(t)$ can be taken as a constant, and in such a case equation (13) can be solved by the Spline collocation method numerically. Define the displacement vector as a 3-D B-spline function

$$(Z_r)_{mn} = \sum_{j=-1}^{m+1} C_{rj} \Omega_3 \left(\frac{t - t_j}{\Delta t} \right), \tag{14}$$

where Z_r $(r = w, x, y)$ correspond to the displacements W, X, Y respectively, Ω_3 is the third order B-spline function, t_j is any Spline node in the time domain, Δt is the time increase.

Substituting equation (14) into equation (13), and letting the residuals to equal zero, one can obtain

$$\mathbf{L}\mathbf{C}_{i+1} + \mathbf{L}_1 \mathbf{C}_i + \mathbf{L}_2 \mathbf{C}_{i-1} + \mathbf{L}_3 \mathbf{C}_{i-2} = \Delta \mathbf{F}(t_i), \tag{15}$$

where

$$\mathbf{L} = \bar{\mathbf{M}}(t_{i-1}) + \bar{\mathbf{C}}(t_{i-1})\Delta t/2 + \bar{\mathbf{K}}(t_{i-1})(\Delta t)^2/6,$$

$$\mathbf{L}_1 = -3\bar{\mathbf{M}}(t_{i-1}) - \bar{\mathbf{C}}(t_{i-1})\Delta t/2 - \bar{\mathbf{K}}(t_{i-1})(\Delta t)^2/2,$$

$$\mathbf{L}_2 = 3\bar{\mathbf{M}}(t_{i-1}) - \bar{\mathbf{C}}(t_{i-1})\Delta t/2 - \bar{\mathbf{K}}(t_{i-1})(\Delta t)^2/2,$$

$$\mathbf{L}_3 = -\bar{\mathbf{M}}(t_{i-1}) + \bar{\mathbf{C}}(t_{i-1})\Delta t/2 - \bar{\mathbf{K}}(t_{i-1})(\Delta t)^2/6,$$

$$\Delta\mathbf{F}(t_i) = \Delta\mathbf{P}(t_{i-1})(\Delta t)^2 \tag{16}$$

from equation (15), $\mathbf{C} = \{C_w, C_x, C_y\}^{\mathrm{T}}$ can easily be calculated with the initial condition. Resubstituting $\mathbf{C} = \{C_w, C_x, C_y\}^{\mathrm{T}}$ into equation (14), as a result, $W_{mn}(t)$, $X_{mn}(t)$ and $Y_{mn}(t)$ can be obtained.

4. NUMERICAL EXAMPLES AND DISCUSSION

Dynamic and chaotic responses of simply supported shear-deformable laminated plates exposed to an oscillating flow in the time domain were investigated. A program was developed for the purpose and many examples have been solved numerically, including the following.

4.1. COMPARISON STUDIES

Four numerical examples for free vibration and transient response of simply supported antisymmetric angle-ply and symmetric cross-ply laminated plates are presented to show the accuracy and efficiency of the present method.

Example 1. To validate the present method, the fundamental natural frequency coefficients $\varpi = (\omega a^2/h)\sqrt{\rho/E_{22}}$ of $(\theta/\text{-}\theta/\ldots)$ antisymmetric angle-ply laminated square plates are compared in Table 1 with the finite element method (FEM) results given by Phan and Reddy [10], using their material properties, i.e., $E_{11}/E_{22} = 40$, $G_{12}/E_{22} = G_{13}/E_{22} = 0{\cdot}6$, $G_{23}/E_{22} = 0{\cdot}5$ and $\nu_{12} = 0{\cdot}25$.

TABLE 1

Fudamental frequency coefficients $\varpi = (\omega a^2/h)\sqrt{\rho/E_{22}}$ *for* $(\theta/\text{-}\theta/\ldots)$ *square plates*

		$\theta = 30$		$\theta = 45$	
a/h		$N = 2$	$N = 6$	$N = 2$	$N = 6$
4	Present	9·5011	10·5818	9·8128	10·899
	Phan & Reddy [10]	9·4456	10·577	9·7594	10·895
10	Present	12·927	18·176	13·311	19·029
	Phan & Reddy [10]	12·873	18·170	13·263	19·025
20	Present	13·869	21·650	14·264	22·879
	Phan & Reddy [10]	13·849	21·648	14·246	22·877
50	Present	14·177	23·068	14·575	24·480
	Phan & Reddy [10]	14·174	23·067	14·572	24·480
100	Present	14·223	23·295	14·621	24·739
	Phan & Reddy [10]	14·223	23·295	14·621	24·739

TABLE 2

The fudamental frequency coefficients $\varpi = (\omega a^2/h)\sqrt{\rho/E_{22}}$ *for a* $(0/90)_s$ *square plate* $(a/h = 5)$ *with different values of* E_{11}/E_{22}

E_{11}/E_{22}	3-D [7]	HSDPT [13]	HSDPT [10]	HSDPT [12]	Present
10	8·2103	8·2940	8·2718	8·2718	8·2718
20	9·5603	9·5439	9·5623	9·5623	9·5623
30	10·272	10·284	10·272	10·272	10·272
40	10·752	10·794	10·787	10·787	10·787

Example 2. We consider now the fundamental natural frequency coefficients of $(0/90)_s$ symmetric cross-ply laminated square plates, which are compared in Table 2 with HSDPT results given by Phan and Reddy [10], Khdeir [12], Khdeir and Librescu [13] and three-dimensional elasticity solutions of Noor [7]. The material properties are the same as used in Example 1.

Example 3. We now turn our attention to the transient response of a (0/90/0) cross-ply laminated square plate with $b/h = 5$ under time-dependent sinusoidal distributed load defined as

$$q = q_0 F(t) \sin\frac{\pi}{a} x \sin\frac{\pi}{b} y, \qquad F(t) = \begin{cases} \sin(\pi t/t_1) & 0 \leqslant t \leqslant t_1, \\ 0 & t > t_1 \end{cases} \tag{17}$$

in which $t_1 = 0{\cdot}006$ s and $q_0 = 68{\cdot}9476$ MPa. All plies are assumed to have the same thickness and plate thickness $h = 0{\cdot}1524$ m. The material properties are: $E_{11} = 172{\cdot}369$ GPa, $E_{22} = 6{\cdot}895$ GPa, $G_{12} = G_{13} = 3{\cdot}448$ GPa, $G_{23} = 1{\cdot}379$ GPa, $\nu_{12} = 0{\cdot}25$ and $\rho = 1603{\cdot}03$ kg/m^3. The variations of the central deflection as functions of time are compared in Figure 1 with HSDPT results of Khdeir and Reddy [18].

Example 4. We now compare the variations of the central deflection as functions of time for a $(\pm 45)_T$ antisymmetric angle-ply laminated square plate subjected to a suddenly applied uniformly distributed load in Figure 2 with the results of Kant *et al.* [17], using their computing data: $E_{11}/E_{22} = 25$, $G_{12}/E_{22} = G_{13}/E_{22} = G_{23}/E_{22} = 0{\cdot}5$, $E_{22} = 21$ GPa, $\nu_{12} = 0{\cdot}25$, $a = b = 0{\cdot}25$ m, $h = 0{\cdot}05$ m, $\rho = 800$ kg/m^3 and $q = 0{\cdot}1$ MPa.

The good agreement between the present results and referenced solutions of Tables 1 and 2, and Figures 1 and 2 reveals the high accuracy of the presented method.

4.2 PARAMETRIC STUDIES

A parametric study of antisymmetric angle-ply and symmetric cross-ply laminated plates exposed to an oscillating flow was carried out. Under the present study, we assume that the fluid velocity has the form $\dot{U} = \dot{U}_m \sin \omega t$, the material properties are: $E_{11} = 203{\cdot}00$ GPa, $E_{22} = 11{\cdot}20$ GPa, $G_{12} = G_{13} = 8{\cdot}40$ GPa, $G_{23} = 4{\cdot}03$ GPa, $\nu_{12} = 0{\cdot}32$ and $\rho = 1600$ kg/m^3. All plies are assumed to have the same thickness and the total thickness of the plate is $h = 0{\cdot}05$ m. The fluid parameters adopted here are $\rho_0 = 1000$ kg/m^3, $\dot{U}_m = 20$ m/s, $\omega = 125$ rad/s, $c_m = 1{\cdot}61$ and $c_D = 1{\cdot}12$. However, the analysis is equally applicable to other types of fluid parameters as well. Zero initial conditions are assumed. Typical results for central deflection as functions of time are shown in Figures 3–7.

Figure 3 shows central deflection as a function of time for a $(0/90)_s$ square plate $(b/h = 10)$ under oscillating flow. It can be found that very complex vibration patterns occur. Due to

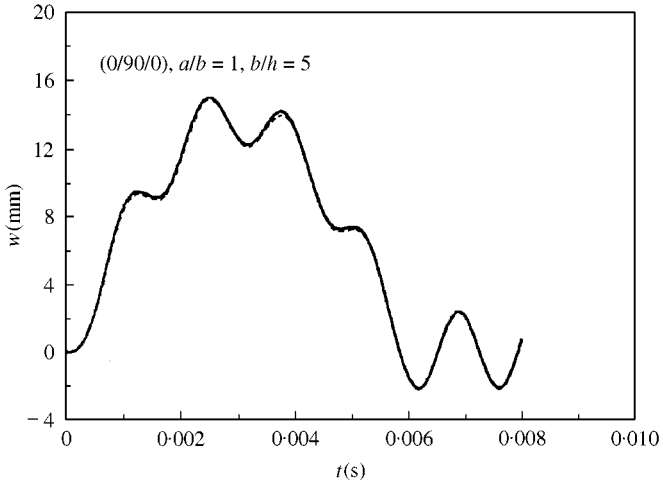

Figure 1. Comparisons of transient response of a (0/90/0) square plate under sinusoidal distributed load: ——, present; - - - - -, Khdeir & Reddy [18].

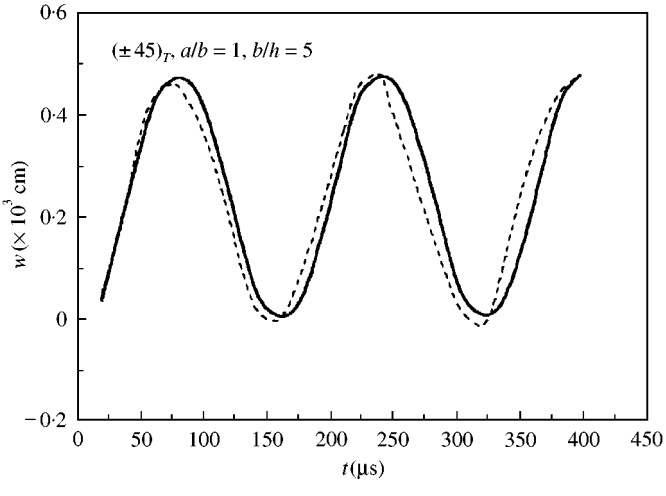

Figure 2. Comparisons of transient response of a $(\pm 45)_T$ square plate subjected to a suddenly applied uniformly distributed load: ——, present; - - - -, Kant *et al.* [17].

fluid damping, the vibration firstly dissipates and then the response amplitude only varies slightly at longer times.

Figure 4 shows the effect of width-to-thickness ratio on the dynamic response of a $(\pm 45_2)_T$ square plate subjected to oscillating flow and the results are compared with their classical countparts (CPT). It can be found that the transverse deflection predicted by HSDPT is larger than that predicted by the CPT. It can also be seen that the transverse deflection of the plate with $b/h = 10$ is much greater than that of the plate with $b/h = 5$.

Figure 5 shows the effect of the total number of plies N on the dynamic response of antisymmetric angle-ply laminated square plates ($b/h = 10$) exposed to oscillating flow. It can be seen that the transverse deflection decreases as the total number of plies N increases, but the effect is very small.

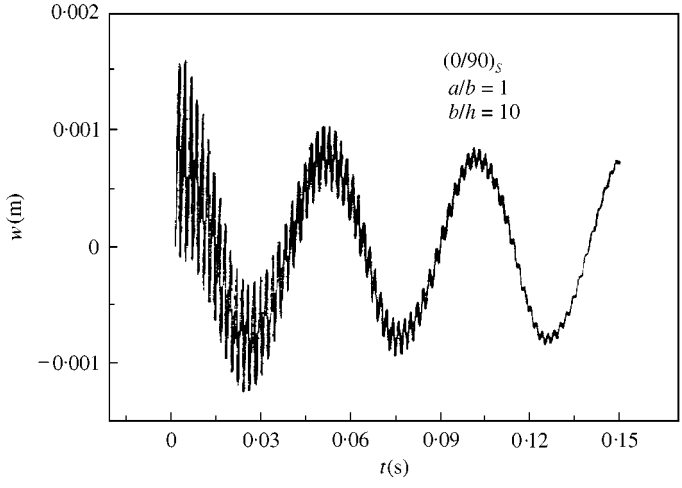

Figure 3. Central deflection versus time for a $(0/90)_s$ square plate exposed to oscillating flow.

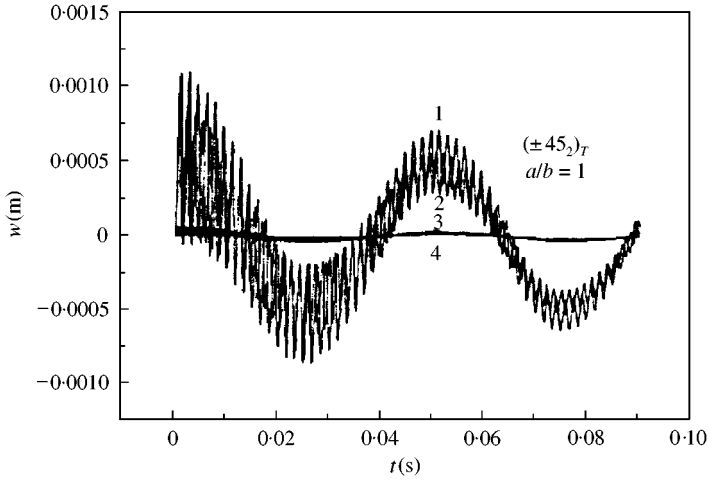

Figure 4. Effect of transverse shear deformation on the dynamic response of a $(\pm 45_2)_T$ plate under oscillating flow: 1, HSDPT $b/h = 10$; 2, CPT $b/h = 10$; 3, HSDPT $b/h = 5$; 4, CPT $b/h = 5$.

Figure 6 compares the variations of the central deflection as functions of time for $(\pm 45_2)_T$ and $(\pm 30_2)_T$ antisymmetric angle-ply laminated square plates ($b/h = 10$). The results show that the transverse central deflection of the $(\pm 45_2)_T$ plate is slightly lower than that of the $(\pm 30_2)_T$ plate.

Figure 7 shows the effect of plate aspect ratio on the dynamic response of $(\pm 45_2)_T$ plates with either $a = b = 0{\cdot}5$ m or $a = 0{\cdot}75$ m, $b = 0{\cdot}5$ m. It can be seen that the transverse deflection of the rectangular plate is much higher than that of the square plate.

Figures 8 and 9 show the phase plane diagrams of forced vibration induced by oscillating flow for $(0/90)_s$ and $(\pm 45_2)_T$ plates with $a/h = b/h = 10$. It can be found that irregular motion now occurs and the phase plane trajectories for these vibrations appear chaotic.

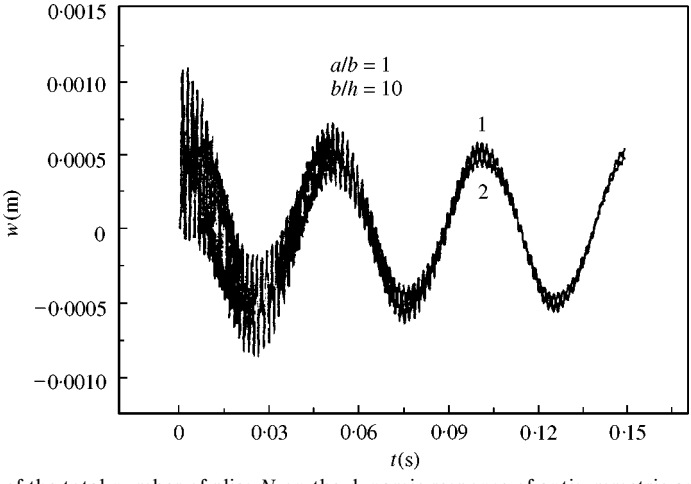

Figure 5. Effect of the total number of plies N on the dynamic response of antisymmetric angle-ply laminated plates under oscillating flow: 1, $(\pm 45_2)_T$; 2, $(\pm 45_5)_T$.

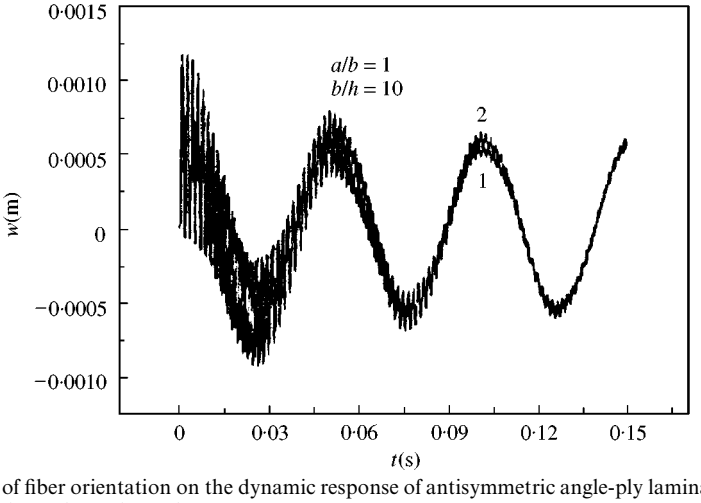

Figure 6. Effect of fiber orientation on the dynamic response of antisymmetric angle-ply laminated plates under oscillating flow: 1, $(\pm 45_2)_T$; 2, $(\pm 30_2)_T$.

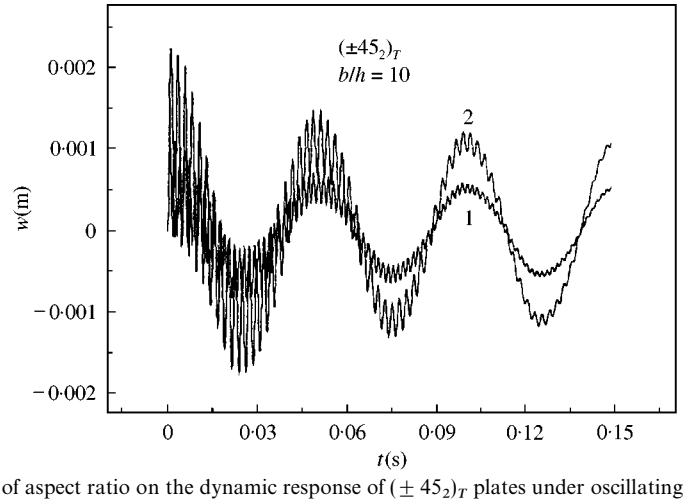

Figure 7. Effect of aspect ratio on the dynamic response of $(\pm 45_2)_T$ plates under oscillating flow: 1, $a/b = 1$; 2, $a/b = 1{\cdot}5$.

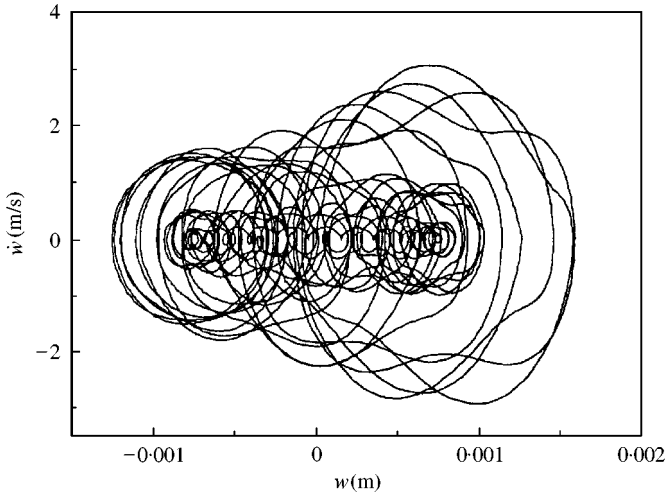

Figure 8. Phase plane trajectories for $(0/90)_s$ plate ($a/h = b/h = 10$) under oscillating flow.

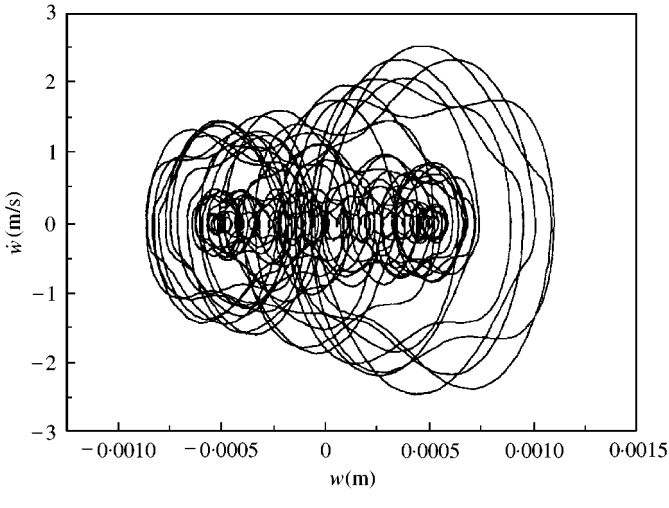

Figure 9. Phase plane trajectories for $(\pm 45_2)_T$ plate ($a/h = b/h = 10$) under oscillating flow.

5. CONCLUDING REMARKS

Dynamic and chaotic behaviors of a simply supported, shear-deformable laminated plate exposed to an oscillating flow have been studied by using an analytical–numerical procedure. A number of issues related to the free vibration and transient response of antisymmetric angle-ply and symmetric cross-ply laminated plates have been examined.

A parametric study of shear-deformable laminated plates in an oscillating flow has been carried out and pertinent conclusions about the influence played in this respect by a number of geometrical and physical parameters have been outlined. The results show that very complex vibration patterns can occur and essentially chaotic motion can develop. They also confirm that the characteristics of dynamic behavior are significantly influenced by transverse shear deformation, plate aspect ratio and fiber orientation. In contrast, the total number of plies has less effect.

REFERENCES

1. K. KUWAHARA 1973 *Journal of Physics Society of Japan* **35**, 1545–1553. Numerical study of flow past an inclined flat plate by an inviscid model.
2. T. SARPKAYA 1975 *Journal of Fluid Mechanics* **68**, 109–128. An inviscid model of two-dimensional vortex shedding for transient and asymptotically steady separated flow over an inclined plate.
3. M. KIYA and M. ARIE 1980 *Bulletin of JSME* **23**, 1451–1459. Discrete-vortex simulation of unsteady separated flow behind a nearly normal plate.
4. R. CHEIN and J. N. CHUNG 1988 *Computers and Fluids* **16**, 405–427. Discrete-vortex simulation of flow over inclined and normal plate.
5. A. OKAJIMA, T. MATSUMOTO and S. KIMURA 1998 *JSME International Journal* Series B **41**, 214–220. Aerodynamic characteristics of flat plates with various angles of attack in oscillatory flow.
6. S. SRINIVAS and A. K. RAO 1970 *International Journal of Solids and Structures* **6**, 1463–1481. Bending, vibration and buckling of simply supported thick orthotropic rectangular plates and laminates.
7. A. K. NOOR 1973 *American Institute of Aeronautics and Astronautics Journal* **11**, 1038–1039. Free vibration of multilayered composite plates.
8. C. W. BERT and T. L. C. CHEN 1978 *International Journal of Solids and Structures* **14**, 465–473. Effect of shear deformation on vibration of antisymmetric angle-ply laminated rectangular plates.
9. J. N. REDDY and N. D. PHAN 1985 *Journal of Sound and Vibration* **98**, 157–170. Stability and vibration of isotropic, orthotropic and laminated plates according to a higher-order shear deformation theory.
10. N. D. PHAN and J. N. REDDY 1985 *International Journal for Numerical Methods in Engineering* **21**, 2201–2219. Analysis of laminated composite plates using a higher-order shear deformation theory.
11. M. DI SCIUVA 1986 *Journal of Sound and Vibration* **105**, 425–442. Bending, vibration and buckling of simply supported thick multilayered orthotropic plates: an evaluation of a new displacement model.
12. A. A. KHDEIR 1988 *Journal of Sound and Vibration* **126**, 447–461. Free vibration and buckling of symmetric cross-ply laminated plates by an exact method.
13. A. A. KHDEIR and L. LIBRESCU 1988 *Composite Structures* **9**, 259–277. Analysis of symmetric cross-ply laminated elastic plates using a higher-order theory: Part II—buckling and free vibration.
14. A. K. GHOSH and S. S. DEY 1994 *Computer and Structures* **53**, 397–404. Free vibration of laminated composite plates—a simple finite element based on higher order theory.
15. C. P. WU and W. Y. CHEN 1994 *Journal of Sound and Vibration* **177**, 503–520. Vibration and stability of laminated plates based on a local higher order plate theory.
16. A. A. KHDEIR and J. N. REDDY 1999 *Computers and Structures* **71**, 617–626. Free vibration of laminated composite plates using second-order shear deformation theory.
17. T. KANT, R. V. RAVICHANDRAN, B. N. PANDYA and MALLIKAJUNA 1988 *Composite Structures* **9**, 319–342. Finite element transient dynamic analysis of isotropic and fibre reinforced composite plates using a higher-order theory.
18. A. A. KHDEIR and J. N. REDDY 1989 *Composites Science and Technology* **34**, 205–224. Exact solutions for the transient response of symmetric cross-ply laminates using a higher-order plate theory.
19. A. A. KHDEIR and J. N. REDDY 1989 *International Journal of Mechanical Sciences* **31**, 499–510. On the forced motions of antisymmetric cross-ply laminated plates.
20. W. HAN and M. PETYT 1996 *Computers and Structures* **61**, 713–724. Linear vibration analysis of laminated rectangular plates using the hierarchical finite element method—II. Forced vibration analysis.
21. J. N. REDDY 1998 *Mechanics of Laminated Composite Plates*: *Theory and Analysis*. Boca Raton, FL: CRC Press.
22. J. R. MORISON 1950 *Petroleum Transactions* **189**, 149–157. The force exerted by surface waves on piles.
23. H. S. SHEN 1997 *Applied Mathematics and Mechanics* **18**, 1137–1152. Kármán-type equations for a higher-order shear deformation plate theory and its use in the thermal post-buckling analysis.
24. H. S. SHEN 1998 *Computers and Structures* **66**, 395–409. Thermomechanical post-buckling analysis of imperfect laminated plates using a higher-order shear deformation theory.

APPENDIX A

In equations (1)–(4)

$$L_{11}(\,) = \frac{4}{3h^2}\left[F_{11}^* \frac{\partial^4}{\partial x^4} + (F_{12}^* + F_{21}^* + 4F_{66}^*)\frac{\partial^4}{\partial x^2 \partial y^2} + F_{22}^* \frac{\partial^4}{\partial y^4}\right],$$

$$L_{12}(\,) = \left[D_{11}^* - \frac{4}{3h^2} F_{11}^*\right]\frac{\partial^3}{\partial x^3} + \left[(D_{12}^* + 2D_{66}^*) - \frac{4}{3h^2}(F_{12}^* + 2F_{66}^*)\right]\frac{\partial^3}{\partial x \partial y^2},$$

$$L_{13}(\,) = \left[(D_{12}^* + 2D_{66}^*) - \frac{4}{3h^2}(F_{21}^* + 2F_{66}^*)\right]\frac{\partial^3}{\partial x^2 \partial y} + \left[D_{22}^* - \frac{4}{3h^2} F_{22}^*\right]\frac{\partial^3}{\partial y^3},$$

$$L_{14}(\,) = (2B_{26}^* - B_{61}^*)\frac{\partial^4}{\partial x^3 \partial y} + (2B_{16}^* - B_{62}^*)\frac{\partial^4}{\partial x \partial y^3},$$

$$L_{21}(\,) = \left[A_{55} - \frac{8}{h^2} D_{55} + \frac{16}{h^4} F_{55}\right]\frac{\partial}{\partial x} + \frac{4}{3h^2}\left[\left(F_{11}^* - \frac{4}{3h^2} H_{11}^*\right)\frac{\partial^3}{\partial x^3} + \left((F_{21}^* + 2F_{66}^*) - \frac{4}{3h^2}(H_{12}^* + 2H_{66}^*)\right)\frac{\partial^3}{\partial x \partial y^2}\right],$$

$$L_{22}(\,) = \left[A_{55} - \frac{8}{h^2} D_{55} + \frac{16}{h^4} F_{55}\right] - \left[D_{11}^* - \frac{8}{3h^2} F_{11}^* + \frac{16}{9h^4} H_{11}^*\right]\frac{\partial^2}{\partial x^2} - \left[D_{66}^* - \frac{8}{3h^2} F_{66}^* + \frac{16}{9h^4} H_{66}^*\right]\frac{\partial^2}{\partial y^2},$$

$$L_{23}(\,) = L_{32}(\,) = \left[(D_{12}^* + D_{66}^*) - \frac{4}{3h^2}(F_{12}^* + F_{21}^* + 2F_{66}^*) + \frac{16}{9h^4}(H_{12}^* + H_{66}^*)\right]\frac{\partial^2}{\partial x \partial y},$$

$$L_{24}(\,) = L_{42}(\,) = \left[(B_{26}^* - B_{61}^*) - \frac{4}{3h^2}(E_{26}^* - E_{61}^*)\right]\frac{\partial^3}{\partial x^2 \partial y} + \left[B_{16}^* - \frac{4}{3h^2} E_{16}^*\right]\frac{\partial^3}{\partial y^3},$$

$$L_{31}(\,) = \left[A_{44} - \frac{8}{h^2} D_{44} + \frac{16}{h^4} F_{44}\right]\frac{\partial}{\partial y} + \frac{4}{3h^2}\left[\left((F_{12}^* + 2F_{66}^*) - \frac{4}{3h^2}(H_{12}^* + 2H_{66}^*)\right)\frac{\partial^3}{\partial x^2 \partial y} + \left(F_{22}^* - \frac{4}{3h^2} H_{22}^*\right)\frac{\partial^3}{\partial y^3}\right],$$

$$L_{33}(\,) = \left[A_{44} - \frac{8}{h^2} D_{44} + \frac{16}{h^4} F_{44}\right] - \left[D_{66}^* - \frac{8}{3h^2} F_{66}^* + \frac{16}{9h^4} H_{66}^*\right]\frac{\partial^2}{\partial x^2} - \left[D_{22}^* - \frac{8}{3h^2} F_{22}^* + \frac{16}{9h^4} H_{22}^*\right]\frac{\partial^2}{\partial y^2},$$

$$L_{34}(\,) = L_{43}(\,) = \left[B_{26}^* - \frac{4}{3h^2} E_{26}^*\right]\frac{\partial^3}{\partial x^3} + \left[(B_{16}^* - B_{62}^*) - \frac{4}{3h^2}(E_{16}^* - E_{62}^*)\right]\frac{\partial^3}{\partial x \partial y^2},$$

$$L_{41}(\,) = A_{22}^{*}\frac{\partial^4}{\partial x^4} + (2A_{12}^{*} + A_{66}^{*})\frac{\partial^4}{\partial x^2 \partial y^2} + A_{11}^{*}\frac{\partial^4}{\partial y^4},$$

$$L_{44}(\,) = \frac{4}{3h^2}\left[(2E_{26}^{*} - E_{61}^{*})\frac{\partial^4}{\partial x^3 \partial y} + (2E_{16}^{*} - E_{62}^{*})\frac{\partial^4}{\partial x \partial y^3}\right], \tag{A1}$$

where $[A_{ij}^{*}]$, $[B_{ij}^{*}]$, $[D_{ij}^{*}]$, $[E_{ij}^{*}]$, $[F_{ij}^{*}]$ and $[H_{ij}^{*}]$ $(i, j = 1, 2, 6)$ are reduced stiffness matrices, defined as

$$\mathbf{A}^{*} = \mathbf{A}^{-1}, \qquad \mathbf{B}^{*} = -\mathbf{A}^{-1}\mathbf{B}, \qquad \mathbf{D}^{*} = \mathbf{D} - \mathbf{B}\mathbf{A}^{-1}\mathbf{B}, \qquad \mathbf{E}^{*} = -\mathbf{A}^{-1}\mathbf{E},$$

$$\mathbf{F}^{*} = \mathbf{F} - \mathbf{E}\mathbf{A}^{-1}\mathbf{B}, \qquad \mathbf{H}^{*} = \mathbf{H} - \mathbf{E}\mathbf{A}^{-1}\mathbf{E}, \tag{A2}$$

where A_{ij}, B_{ij}, etc., are the plate stiffnesses, defined by

$$(A_{ij}, B_{ij}, D_{ij}, E_{ij}, F_{ij}, H_{ij}) = \sum_{k=1}^{} \int_{h_k - 1}^{h_k} (\bar{Q}_{ij})_k (1, z, z^2, z^3, z^4, z^6)\,\mathrm{d}z \quad (i, j = 1, 2, 6), \tag{A3a}$$

$$(A_{ij}, D_{ij}, F_{ij}) = \sum_{k=1}^{} \int_{h_k - 1}^{h_k} (\bar{Q}_{ij})_k (1, z^2, z^4)\,\mathrm{d}z \quad (i, j = 4, 5), \tag{A3b}$$

where $\bar{Q}_{ij}$ are the transformed elastic constants, defined by

$$\begin{pmatrix} \bar{Q}_{11} \\ \bar{Q}_{12} \\ \bar{Q}_{22} \\ \bar{Q}_{16} \\ \bar{Q}_{26} \\ \bar{Q}_{66} \end{pmatrix} = \begin{pmatrix} c^4 & 2c^2s^2 & s^4 & 4c^2s^2 \\ c^2s^2 & c^4 + s^4 & c^2s^2 & -4c^2s^2 \\ s^4 & 2c^2s^2 & c^4 & 4c^2s^2 \\ c^3s & cs^3 - c^3s & -cs^3 & -2cs(c^2 - s^2) \\ cs^3 & c^3s - cs^3 & -c^3s & 2cs(c^2 - s^2) \\ c^2s^2 & -2c^2s^2 & c^2s^2 & (c^2 - s^2)^2 \end{pmatrix} \begin{pmatrix} Q_{11} \\ Q_{12} \\ Q_{22} \\ Q_{66} \end{pmatrix} \tag{A4a}$$

and

$$\begin{pmatrix} \bar{Q}_{44} \\ \bar{Q}_{45} \\ \bar{Q}_{55} \end{pmatrix} = \begin{pmatrix} c^2 & s^2 \\ -cs & cs \\ s^2 & c^2 \end{pmatrix} \begin{pmatrix} Q_{44} \\ Q_{55} \end{pmatrix}, \tag{A4b}$$

where

$$Q_{11} = \frac{E_{11}}{(1 - \nu_{12}\nu_{21})}, \qquad Q_{22} = \frac{E_{22}}{(1 - \nu_{12}\nu_{21})}, \qquad Q_{12} = \frac{\nu_{21}E_{11}}{(1 - \nu_{12}\nu_{21})},$$

$$Q_{44} = G_{23}, \qquad Q_{55} = G_{13}, \qquad Q_{66} = G_{12} \tag{A4c}$$

in which E_{11}, E_{22}, G_{12}, G_{13}, G_{23}, ν_{12} and ν_{21} have their usual meanings, and

$$c = \cos\theta, \quad s = \sin\theta, \tag{A4d}$$

where θ = lamination angle with respect to the plate x-axis. Also

$$I_{11} = I_1,$$

$$I_{12} = \left[\left(\frac{4}{3h^2}\right)^2 I_7 + \frac{4}{3h^2}\bar{I}_5 - \left(\frac{4}{3h^2} I_4 + \bar{I}_2\right)\frac{4}{3h^2}\frac{I_4}{I_1}\right],$$

$$I_{13} = \left[\left(\frac{4}{3h^2} I_4 + \bar{I}_2\right)\frac{\bar{I}_2}{I_1} - \left(\frac{4}{3h^2}\bar{I}_5 + \bar{I}_3\right)\right],$$

$$I_{21} = \left[\frac{4}{3h^2}\bar{I}_5 - \frac{4}{3h^2}\frac{\bar{I}_2 I_4}{I_1}\right], \qquad I_{22} = \left[\frac{(\bar{I}_2)^2}{I_1} - \bar{I}_3\right],$$

$$I_{31} = I_{21}, \qquad I_{32} = I_{22}, \tag{A5a}$$

where

$$\bar{I}_2 = I_2 - \frac{4}{3h^2} I_4, \qquad \bar{I}_5 = I_5 - \frac{4}{3h^2} I_7, \qquad \bar{I}_3 = I_3 - \frac{8}{3h^2} I_5 + \frac{16}{9h^4} I_7. \tag{A5b}$$

The inertias I_i ($i = 1$–$5, 7$) are defined by

$$(I_1, I_2, I_3, I_4, I_5, I_7) = \sum_{k=1}^{N} \int_{h_k - 1}^{h_k} \rho^{(k)}(1, z, z^2, z^3, z^4, z^6)\,\mathrm{d}z, \tag{A6}$$

where $\rho^{(k)}$ is the mass density of the kth layer.

APPENDIX B

In equation (10)

$$g_1 = \frac{(-4/3h^2)[(2E^*_{26} - E^*_{61})\alpha^3\beta + (2E^*_{16} - E^*_{62})\alpha\beta^3]}{A^*_{22}\alpha^4 + (2A^*_{12} + A^*_{66})\alpha^2\beta^2 + A^*_{11}\beta^4},$$

$$g_2 = \frac{[(B^*_{26} - B^*_{61}) - (4/3h^2)(E^*_{26} - E^*_{61})]\alpha^2\beta + [B^*_{16} - (4/3h^2)E^*_{16})]\beta^3}{A^*_{22}\alpha^4 + (2A^*_{12} + A^*_{66})\alpha^2\beta^2 + A^*_{11}\beta^4},$$

$$g_3 = \frac{[B^*_{26} - (4/3h^2)E^*_{26}]\alpha^3 + [(B^*_{16} - B^*_{62}) - (4/3h^2)(E^*_{16} - E^*_{62})]\alpha\beta^2}{A^*_{22}\alpha^4 + (2A^*_{12} + A^*_{66})\alpha^2\beta^2 + A^*_{11}\beta^4}. \tag{B1}$$

APPENDIX C

In equation (12), for two cases of $(\dot{U} - \dot{w}) \geqslant 0$ and $(\dot{U} - \dot{w}) < 0$

$$f_1(t) = \operatorname{sgn}\rho_0 c_D \dot{U}, \qquad f_2(t) = \frac{16}{mn\pi^2}\rho_0 h c_m \ddot{U}, \qquad f_3(t) = \operatorname{sgn}\frac{8}{mn\pi^2}\rho_0 c_D \dot{U}^2,$$

$$a_1 = -\operatorname{sgn}\frac{32\rho c_D}{9mn\pi^2}, \tag{C1}$$

where sgn is the signal function of $(\dot{U} - \dot{w})$, and

$$K_{11} = \frac{4}{3h^2}[F_{11}^*\alpha^4 + (F_{12}^* + F_{21}^* + 4F_{66}^*)\alpha^2\beta^2 + F_{22}^*\beta^4] - [2B_{26}^* - B_{61}^*]g_1\alpha^3\beta$$
$$- (2B_{16}^* - B_{62}^*)g_1\alpha\beta^3,$$

$$K_{12} = -\left[\left(D_{11}^* - \frac{4}{3h^2}F_{11}^*\right)\alpha^3 + \left((D_{12}^* + 2D_{66}^*) - \frac{4}{3h^2}(F_{12}^* + 2F_{66}^*)\right)\alpha\beta^2\right.$$
$$\left. + (2B_{26}^* - B_{61}^*)\alpha^3\beta g_2 + (2B_{16}^* - B_{62}^*)\alpha\beta^3 g_2\right],$$

$$K_{13} = -\left[\left((D_{12}^* + 2D_{66}^*) - \frac{4}{3h^2}(F_{21}^* + 2F_{66}^*)\right)\alpha^2\beta\right.$$
$$\left. + \left(D_{22}^* - \frac{4}{3h^2}F_{22}^*\right)\beta^3 + (2B_{26}^* - B_{61}^*)\alpha^3\beta g_3 + (2B_{16}^* - B_{62}^*)\alpha\beta^3 g_3\right],$$

$$K_{21} = \left[A_{55} - \frac{8}{h^2}D_{55} + \frac{16}{h^4}F_{55}\right]\alpha$$
$$- \frac{4}{3h^2}\left[\left(F_{11}^* - \frac{4}{3h^2}H_{11}^*\right)\alpha^3 + \left((F_{21}^* + 2F_{66}^*) - \frac{4}{3h^2}(H_{12}^* + 2H_{66}^*)\right)\alpha\beta^2\right]$$
$$+ \left[(B_{26}^* - B_{61}^*) - \frac{4}{3h^2}(E_{26}^* - E_{61}^*)\right]\alpha^2\beta g_1 + \left[B_{16}^* - \frac{4}{3h^2}E_{16}^*\right]\beta^3 g_1,$$

$$K_{22} = \left[A_{55} - \frac{8}{h^2}D_{55} + \frac{16}{h^4}F_{55}\right] + \left[D_{11}^* - \frac{8}{3h^2}F_{11}^* + \frac{16}{9h^4}H_{11}^*\right]\alpha^2$$
$$+ \left[D_{66}^* - \frac{8}{3h^2}F_{66}^* + \frac{16}{9h^4}H_{66}^*\right]\beta^2 + \left[(B_{26}^* - B_{61}^*) - \frac{4}{3h^2}(E_{26}^* - E_{61}^*)\right]\alpha^2\beta g_2$$
$$+ \left[B_{16}^* - \frac{4}{3h^2}E_{16}^*\right]\beta^3 g_2,$$

$$K_{23} = \left[(D_{12}^* + D_{66}^*) - \frac{4}{3h^2}(F_{12}^* + F_{21}^* + 2F_{66}^*) + \frac{16}{9h^4}(H_{12}^* + H_{66}^*)\right]\alpha\beta$$
$$+ \left[(B_{26}^* - B_{61}^*) - \frac{4}{3h^2}(E_{26}^* - E_{61}^*)\right]\alpha^2\beta g_3 + \left[B_{16}^* - \frac{4}{3h^2}E_{16}^*\right]\beta^3 g_3,$$

$$K_{31} = \left[A_{44} - \frac{8}{h^2}D_{44} + \frac{16}{h^4}F_{44}\right]\beta$$
$$- \frac{4}{3h^2}\left[\left(F_{12}^* + 2F_{66}^*\right) - \frac{4}{3h^2}(H_{12}^* + 2H_{66}^*)\right)\alpha^2\beta + \left(F_{22}^* - \frac{4}{3h^2}H_{22}^*\right)\beta^3\right]$$
$$+ \left[B_{26}^* - \frac{4}{3h^2}E_{26}^*\right]\alpha^3 g_1 + \left[(B_{16}^* - B_{62}^*) - \frac{4}{3h^2}(E_{16}^* - E_{62}^*)\right]\alpha\beta^2 g_1,$$

$$K_{32} = \left[(D^*_{12} + D^*_{66}) - \frac{4}{3h^2}(F^*_{12} + F^*_{21} + 2F^*_{66}) + \frac{16}{9h^4}(H^*_{12} + H^*_{66}) \right] \alpha\beta$$
$$+ \left[B^*_{26} - \frac{4}{3h^2} E^*_{26} \right] \alpha^3 g_2 + \left[(B^*_{16} - B^*_{62}) - \frac{4}{3h^2}(E^*_{16} - E^*_{62}) \right] \alpha\beta^2 g_2,$$

$$K_{33} = \left[A_{44} - \frac{8}{h^2} D_{44} + \frac{16}{h^4} F_{44} \right] + \left[D^*_{66} - \frac{8}{3h^2} F^*_{66} + \frac{16}{9h^4} H^*_{66} \right] \alpha^2$$
$$+ \left[D^*_{22} - \frac{8}{3h^2} F^*_{22} + \frac{16}{9h^4} H^*_{22} \right] \beta^2 + \left[B^*_{26} - \frac{4}{3h^2} E^*_{26} \right] \alpha^3 g_3$$
$$+ \left[(B^*_{16} - B^*_{62}) - \frac{4}{3h^2}(E^*_{16} - E^*_{62}) \right] \alpha\beta^2 g_3,$$

$$M_{11} = I_1 + \left[\left(\frac{4}{3h^2} \right)^2 I_7 + \frac{4}{3h^2} \bar{I}_5 - \left(\frac{4}{3h^2} I_4 + \bar{I}_2 \right) \frac{4}{3h^2} \frac{I_4}{I_1} \right] (\alpha^2 + \beta^2) + \rho_0 h c_I,$$

$$M_{12} = \left[\left(\frac{4}{3h^2} I_4 + \bar{I}_2 \right) \frac{\bar{I}_2}{I_1} - \left(\frac{4}{3h^2} \bar{I}_5 + \bar{I}_3 \right) \right] \alpha,$$

$$M_{13} = \left[\left(\frac{4}{3h^2} I_4 + \bar{I}_2 \right) \frac{\bar{I}_2}{I_1} - \left(\frac{4}{3h^2} \bar{I}_5 + \bar{I}_3 \right) \right] \beta,$$

$$M_{21} = \left[\frac{4}{3h^2} \frac{\bar{I}_2 I_4}{I_1} - \frac{4}{3h^2} \bar{I}_5 \right] \alpha,$$

$$M_{22} = \left[\bar{I}_3 - \frac{(\bar{I}_2)^2}{I_1} \right],$$

$$M_{31} = \left[\frac{4}{3h^2} \frac{\bar{I}_2 I_4}{I_1} - \frac{4}{3h^2} \bar{I}_5 \right] \beta,$$

$$M_{23} = M_{32} = 0, \qquad M_{33} = M_{22}. \tag{C2}$$

APPENDIX D

In equation (13)

$$\bar{\mathbf{M}} = \begin{pmatrix} M_{11} & M_{12} & M_{13} \\ M_{21} & M_{22} & 0 \\ M_{31} & 0 & M_{33} \end{pmatrix}, \qquad \bar{\mathbf{C}}(t) = \begin{pmatrix} f_1(t) + 2a_1 \dot{W}_{mn}(t) & 0 & 0 \\ 0 & 0 & 0 \\ 0 & 0 & 0 \end{pmatrix},$$

$$\bar{\mathbf{K}} = \begin{pmatrix} K_{11} & K_{12} & K_{13} \\ K_{21} & K_{22} & K_{23} \\ K_{31} & K_{32} & K_{33} \end{pmatrix}, \qquad \Delta\mathbf{P}(t) = \begin{pmatrix} \dot{f}_2(t)\Delta t + \dot{f}_3(t)\Delta t - \dot{W}_{mn}(t)\, \dot{f}_1(t)\Delta t \\ 0 \\ 0 \end{pmatrix}. \tag{D1}$$